Polymer−Inorganic Coatings Containing Nanosized Sorbents Selective to Radionuclides. 2. Latex/Tin Oxide Composites for Cobalt Fixation

Svetlana Bratskaya,*,† Alexander Mironenko,† Risto Koivula,‡ Alla Synytska,§,‖ Anna Musyanovych,⊥,# Frank Simon,§ Dmitry Marinin,† Michael Göbel,§ Risto Harjula,‡ and Valentin Avramenko†

†Institute of Chemistry Far Eastern Branch of the Russian Academy of Sciences, 159 ave 100-letiya Vladivostoka, 690022 Vladivostok, Russia

‡University of Helsinki, A. I. Virtasenaukio 1, 00560 Helsinki, Finland

§Leibniz-Institut für Polymerforschung Dresden e.V., Hohe Strasse 6, 01069 Dresden, Germany

‖Technische Universität Dresden, Physikalische Chemie Polymerer Materialen, 01062 Dresden, Germany

⊥Max Planck Institute for Polymer Research, Ackermannweg 10, 55128 Mainz, Germany

#Fraunhofer ICT-IMM, Carl-Zeiss-Strasse 18-20, 55129 Mainz, Germany

Ⓢ Supporting Information

ABSTRACT: Colloidal tin oxide with an average particle size of 3.5 nm, which was ex-situ synthesized by the sol−gel method, has been attached to the surface of amino-functionalized poly(acrylate-co-silane) latex particles with a diameter of 100 nm to yield a composite with selective sorption properties toward Co^{2+} ions. Electrokinetic properties and the colloidal stability of the synthesized latex/SnO_2 composites have been evaluated in dependence on SnO_2 content and pH; the sorption capacity and distribution coefficients of composites for Co^{2+} ions were in accordance with the SnO_2 content and its sorption performance as an individual compound. Composite coatings obtained by casting

latex/SnO_2 dispersions on quartz sand spiked with ^{57}Co radionuclide have efficiently eliminated radionuclides migration from the surface when the SnO_2 volume fraction in the film was 3.5−4.7%. Furthermore, at these SnO_2 loadings, the composite coatings retained the coherent structure of the original latex coating with SnO_2 particles homogeneously distributed over the film thickness. The presence of competing Ca^{2+} ions in the leaching media at a concentration of above 0.01 mol/L results in a decrease of the distribution coefficients of the latex/SnO_2 composite and significantly higher ^{57}Co leaching. The value of the distribution coefficient of the sorption material to be used in latex composite coatings to prevent migration of radionuclides shall be close to 10^6 mL/g.

KEYWORDS: nanoparticles, ^{57}Co, SnO_2, radionuclide migration, soil, dust suppressor
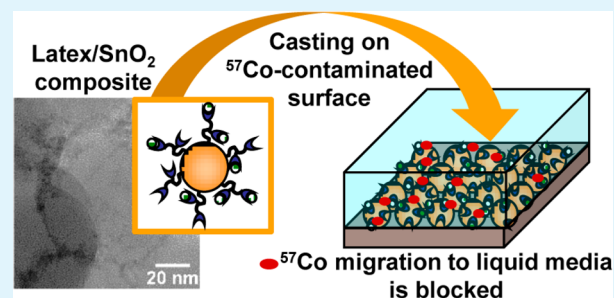
1. INTRODUCTION

Soil can be considered as the main reservoir for artificial radionuclides originated from atmospheric nuclear weapons tests and nuclear power plant accidents.[1,2] Besides, radioactive contamination of the environment can happen as a result of dirty bombs terrorist attacks,[3] explosions, and fires in industry and in transportation of sealed radiation sources. Sealed sources are typically highly radioactive devices having activities of TBq scale where the radioactive isotope is encapsulated, so that under normal operation conditions it is safely isolated from the surrounding by the protective sealing. In the case of an explosion and fire or cutting through the source sealing, radioactivity can spread to the environment and cause local radioactive contamination. Although, in contrast to cesium and strontium, cobalt radionuclides are not considered among the main contributors to radioactive pollutions after accidents at

nuclear power plants, they are very common in industry, medical practice, and research and, due to these reasons, are also more likely to be used in dirty bombs.[3] Cobalt radionuclides are strong γ-emitters, whose release from the sealed sources poses a serious health risk for humans and animals. This determines a sustained interest to the fate of cobalt radionuclides in the environment, sorption/desorption on soil components, and bioavailability.[1,4,5]

Independently of which strategy will be used for remediation of a radioactively contaminated site, it is imperative to eliminate or reduce migration of the radionuclides until cleanup is completed or until the radiation has decayed back to acceptable

levels.[6] In order to prevent radionuclides spreading from a contaminated surface with aerosols, application of polymeric or emulsion fixatives (dust suppressors) became a general practice after nuclear accidents. These formulations are typically casted or spray dried on the contaminated surface within the first hours after the accident to form coatings allowing radionuclides fixation within the top thin layer of the soil or ground.[3] This measure helps to reduce radionuclides migration from the surface with aerosols; however, substantial improvement is still required to eliminate water permeability of fixative coatings and limit radionuclides migration downward to the soil profile with groundwater and atmospheric precipitates. This is a crucial step in reducing the volume of soil to be removed or cleaned after nuclear accidents.[3,6]

We have recently shown that the permeability of fixative latex coatings to cesium radionuclides can be significantly reduced if latex/selective sorbent (cobalt hexacyanoferrate) nanocomposites were used for coatings fabrication.[7] In such materials the film-forming properties of the latex are combined with the sorption properties of inorganic material allowing entrapment of radionuclides in the dust-suppressing film even under permanent contact with liquid media. The aim of the present work was to demonstrate that the same approach can be generalized to fixation of other radionuclides using appropriate selective sorbents for composite fabrication. While transition metal hexacyanoferrates are highly selective to cesium ions,[8] tin oxide shows selective sorption properties toward transition metals such as cobalt[9−11] and nickel[9] ions and can be considered as a promising candidate for fabrication of latex/inorganic composite coatings for fixation of these radionuclides on contaminated surface and prevention of their further migration with atmospheric precipitates and ground waters.

2. EXPERIMENTAL SECTION

2.1. Chemicals and Reagents and Latex Synthesis. Latex synthesis is described in detail in ref 7. The BMADS-0.3 latex poly(methyl methacrylate-co-butyl acrylate-co-diethoxy(methyl)vinyl silane-co-aminoethyl methacrylate) was characterized by an electrokinetic potential (ζ) of +25 ± 7 mV and a particle size of 110 ± 13 nm (pH 6.4, 10^{-4} M KCl). The number of $-NH_2$ groups per latex particle determined by colloid titration[12] was 36 790.

2.2. SnO2 Synthesis. SnO_2 was synthesized using the conventional sol−gel method,[11] where $SnCl_4$ was dissolved in 6 M HCl, and then SnO_2 was precipitated by raising the pH to 3 using 25% ammonia. The precipitate was then washed with distilled water until the water became turbid after 12 h settling time. The precipitate was then placed in a dialysis tube (Visking tube 12−14 kDa), and the tube was placed in a beaker, where fresh ammonia solution (pH 10) was circulated, until the precipitate became a clear solution. The content of tin oxide in the dispersion was 3%.

2.3. Composites and Coatings Preparation. To obtain composites, a predetermined volume of SnO_2 dispersion was added into a latex dispersion with the solid content 2% at pH 5.1 ± 0.1. Composites were labeled as BMADS-0.3/SnO_2 or BMADS-0.3/SnO_2-w, where w is the content of SnO_2 as milligrams per 1 g of dry latex. Coatings were obtained by casting BMADS-0.3/SnO_2 composite dispersions on the silicon wafer or ^{57}Co-spiked quartz sand as described in ref 7. The volume fraction of SnO_2 (φ) in composite coatings was calculated according to the following formula

$$\phi = \frac{W_{SnO2} \cdot V_l \cdot C_l}{h_{film} \cdot S_{film} \cdot \rho_{SnO2}} \cdot 100\%$$

where W_{SnO2} is the content of SnO_2 in composite, g(SnO_2) per 1 g of the dry latex, C_l is the latex solid content in composite dispersion, g/L, V_l is the casted volume of the latex/SnO_2 composite dispersion, L, h_{film}

is the coating (film) thickness, cm, S_{film} is the film area, cm^2, and ρ_{SnO2} is the SnO_2 density (2.02 g/cm^3).

2.4. Characterization of the Latex, SnO2, and Latex/SnO2 Composites. The size and electrokinetic potential of the particles were determined using ZetaSizer Nano ZS analyzer (Malvern Instruments Ltd., Malvern, U.K.).

The morphology of coatings was characterized by means of electron microscopy. A cross-section of the polymer layer was prepared in the form of a simple cut and in the form of a thin lamella by the focused ion beam (NEON40, Carl Zeiss Microscopy GmbH, Oberkochen, Germany) lift-out method after an approximately 100 nm platinum layer was sputtered on the surface (SCD 500 coater, Leica Microsystems GmbH, Wetzlar, Germany). The simple cut was imaged in a scanning electron microscope (SEM, NEON40). The thin lamella was imaged in a transmission electron microscope (TEM, Libra200, Carl Zeiss Microscopy GmbH, Oberkochen, Germany).

2.4.1. X-ray Photoelectron Spectroscopy (XPS). BMADS-0.3/SnO_2-50 composite coating on silicon wafer was introduced in the vacuum system of the Axis Ultra X-ray photoelectron spectrometer (Kratos Analytical, Manchester, U.K.). The spectrometer was equipped with a monochromatic Al Kα ($h\nu$ = 1486.6 eV) X-ray source of 300 W at 15 kV. The kinetic energy of photoelectrons was determined with a hemispheric analyzer set to a pass energy of 160 eV for the wide-scan spectrum and 20 eV for the C 1s high-resolution spectrum. During all measurements electrostatic charging of the sample was avoided by means of a low-energy electron source working in combination with a magnetic immersion lens. Later, all recorded peaks were shifted by the same value that was necessary to set the C 1s peak to 285.00 eV. For the C 1s region the maximum information depth of the XPS method was not more than 8 nm. Quantitative elemental compositions were determined from peak areas using experimentally determined sensitivity factors and the spectrometer transmission function. Spectrum background was subtracted according to the Shirley method. The high-resolution C 1s spectrum was deconvoluted by means of the Kratos spectra deconvolution software. Free parameters of component peaks were their binding energy, height, full width at half-maximum, and the Gaussian−Lorentzian ratio.

2.5. Determination of Distribution Coefficients and Sorption Capacity. Sorption isotherms were obtained by the batch method: an aliquot of BMADS-0.3/SnO_2-50 composite or SnO_2 dispersion was added to $CoCl_2$ solutions in 0.01 M acetate buffer (CH_3COOH/ CH_3COONa, pH 5) so that the solid content in dispersion was 0.05%. After gentle shaking for 18 h, SnO_2 or composite particles were separated by centrifugation (at 30 000 rpm, 30 min), the content of cobalt in supernatant was determined by the atomic spectroscopy method using a Solaar 6 M spectrometer (Thermo Fisher Scientific, Waltham, MA). Sorption capacities in both cases were calculated relative to the weight of SnO_2.

The distribution coefficients (K_d) for SnO_2 and BMADS-0.3/SnO_2-30 composite have been determined in water and 0.5, 0.1, 0.01, and 0.001 M $CaCl_2$ solutions using the ^{57}Co-tracer method: latex/SnO_2 composite or SnO_2 dispersion in solutions with pH 5 were traced with ^{57}Co, and initial γ-activities (~120 Bq/mL) of the dispersions were measured using gamma counter WIZARD 1470 (PerkinElmer, Inc., Waltham, MA). After gentle shaking of the dispersion for 18 h, solid particles were separated by centrifugation (30 000 rpm, 30 min) and γ-activities of supernatants (A_l) were measured by the same method. The γ-activity of the solid phase (A_s) was calculated as a difference between the initial total activity of the sample and the measured activity of the supernatant (A_l).

K_d values were calculated according to the formula $K_d = A_s/A_l \cdot V/m$, where A_s and A_l are the ^{57}Co γ-activities in the solid and liquid phase, respectively, V is the liquid-phase volume (10 mL), and m is the the weight of the composite (0.005 g) or SnO_2 (0.00015 g).

2.6. ^{57}Co Leaching Test. Samples for leaching tests were prepared as described in ref 7 using ^{57}Co. In brief, 60−70 mg of quartz sand (fraction 0.100−0.315 mm) spiked with ^{57}Co (resulting γ-activity ≈ 2000 Bq/g) was homogeneously distributed over a 5.29 cm^2 piece of a double-sided adhesive tape attached to a Petri dish. The coatings on

the sand surfaces were formed as described in section 2.3 and dried for 24 h prior to ^{57}Co leaching experiments. The initial γ-activity of each sample was measured by the direct spectrometric method from the line $E\gamma$ = 122 keV using a γ-ray spectrometer with the germanium detector (Canberra Corp., Meriden, CT). Then 20 mL of distilled water or CaCl$_2$ solution was introduced into the Petri dish and left without shaking for 1000 min (or for the fixed time from 10 min to 6 days in kinetics study). The ^{57}Co distribution between the leaching solution and the solid phase was monitored by measuring the γ-activity of the liquid using gamma counter WIZARD 1470 (PerkinElmer, Inc., Waltham, MA). The amount of ^{57}Co leached from the sand surface (L) was estimated as

$$L = (A_{\text{leached}}/A_0)\cdot 100\%$$

where A_0 is the initial total γ-activity of the solid sample and A_{leached} is the total γ-activity of the solid sample after leaching.

The experimental error of γ-activity measurements was close to 0.3%. For low residual γ-activity (high L values) the counting time was increased to reach the required accuracy.

3. RESULTS AND DISCUSSION

3.1. Fabrication and Properties of Latex/SnO$_2$ Composites.

The general concept of the suggested approach to eliminate migration of radionuclides in the environment after nuclear accidents was previously reported in ref 7. BMADS-0.3/SnO$_2$ composites have been fabricated via electrostatic attachment of ex-situ-synthesized colloidal SnO$_2$ to the surface of amino latex that was possible due to the opposite charge of these nanoparticles in the pH range 3.5−7.5 (Figure 1). However, the pH interval, where stable BMADS-0.3/SnO$_2$ composites can be formed, is narrowed by aggregation of SnO$_2$ nanoparticles at pH < 5 (Figure S1, Supporting Information).
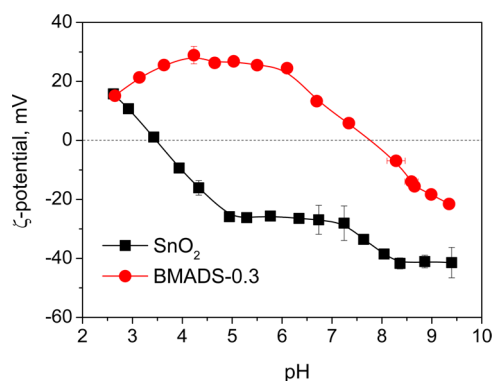

Figure 1. Dependence of electrokinetic potential values (ζ-potential) of BMADS-0.3 latex and colloidal SnO$_2$ on pH.

Once composite was formed, aggregation of SnO$_2$ was suppressed and composite remained colloidally stable over the broader pH range than pure SnO$_2$ (Figure 2A). The TEM image of the aminolatex/SnO$_2$ composite (Figure S2, Supporting Information) shows that SnO$_2$ nanoparticles form on the latex surface in thin irregular layer. The stability of BMADS-0.3/SnO$_2$ composites decreased when the content of SnO$_2$ added to the latex dispersion was above 50 mg per 1 g of dry latex particles, as indicated by a sharp increase of the composite particle size (Figure 2B) and precipitation of SnO$_2$ (Figure S2, Supporting Information).

At maximum packing density, the surface of a sphere with a diameter of 98 nm (latex) can accommodate 2463 particles with a diameter of 3.5 nm (SnO$_2$). At the same time, simple calculations for the BMADS-0.3/SnO$_2$-50 composite give a value of 521 particles of SnO$_2$ per latex particle. Thus, the surface coverage, at which the colloidal stability of the BMADS-0.3/latex system drops due to heterocoagulation, is about 20% (see the Supporting Information for details of the calculations). It is worth mentioning that SnO$_2$ shows a strong tendency to formation of large aggregates of primary SnO$_2$ particles even in alkaline media as illustrated by TEM imaging and the particle size distribution (Figure S3, Supporting Information). Thus, at higher surface coverage, interparticle interactions between SnO$_2$ can contribute to destabilization of the composite via bridging neighboring latex particles.

The sorption properties of BMADS-0.3/SnO$_2$ toward ^{57}Co radionuclides composite are determined only by the presence of SnO$_2$. Data in Table 1 show that the BMADS latex does not efficiently bind ^{57}Co, since, independently of the concentration of competing ions, its K_d values are extremely low. Comparison of K_d values for colloidal SnO$_2$ and BMADS-0.3/SnO$_2$ shows that binding to the latex does not negatively influence the sorption performance of SnO$_2$. In both cases the distribution coefficients decrease with an increase of calcium ion concentration (Table 1). It should be also mentioned that composites as well as colloidal SnO$_2$ show a tendency to strong aggregation at a Ca^{2+} concentration of 0.01 M and higher (Figure S4, Supporting Information). The sorption capacities toward Co^{2+} ions of SnO$_2$ alone and in composite are very close, 0.36 ± 0.04 and 0.31 ± 0.01 mmol/g, respectively (Figure S5, Supporting Information), and in the range reported previously for tin oxide.[10]

3.2. Fabrication and Properties of BMADS-0.3/SnO$_2$ Composite Coatings.

Casting of BMADS-0.3 and BMADS-0.3/SnO$_2$ composite dispersions (latex contents 2%) resulted in formation of coatings with a thickness of about 4 μm. Embedding of SnO$_2$ into the latex film lead to an increase of surface roughness from 0.18 to 0.45 μm and hydrophilicity. The advancing contact angle (θ_{adv}), measured as described in ref 7, decreased from 54° for original latex to 30° for BMADS-0.3/SnO$_2$-50 composite coatings. However, it seems that the presence of SnO$_2$ particles does not hinder latex coalescence and formation of flaw-free coherent coatings (Figure S6, Supporting Information).

XPS investigation of the surface of BMADS-0.3/SnO$_2$-50 composite coating (Figure 3) revealed that the majority of the photoelectrons contributed to the element peaks of carbon (C 1s peak), oxygen (O 1s and O 2s peaks), and silicon (Si 2p and Si 2s peaks) resulted from the elements of the polymer matrix. Tin was detected as the Sn 3p duplet consisting of the Sn 3p$_{3/2}$ and Sn 3p$_{1/2}$ peaks and Sn 3d duplet consisting of the Sn 3d$_{5/2}$ and Sn 3d$_{3/2}$ peaks. Furthermore, the couple of Sn MNN Auger peaks (Sn M$_5$N$_{45}$N$_{45}$ and Sn M$_4$N$_{45}$N$_{45}$) arose in the region of 1049−1058 eV. The shape of the C 1s high-resolution spectrum (Figure S7, Supporting Information) confirms the assumed chemical structure of BMADS-0.3 latex.

Although the presence of SnO$_2$ particles in the top layer (8 nm depth) of BMADS-0.3/SnO$_2$-50 coating was confirmed by XPS, the charge-contrast SEM image shows that there is no nanoparticle-rich zone at the surface (Figure 4A), which is usually formed due to the convective flow transport of nanoparticles to the evaporating meniscus during drying of composite latex/inorganic particles coatings.[13] Instead, cross-section TEM analysis reveals formation of SnO$_2$ nanoparticles network over the full coating thickness (Figure 4B). It is most likely that binding to the latex surface prevents SnO$_2$ migration
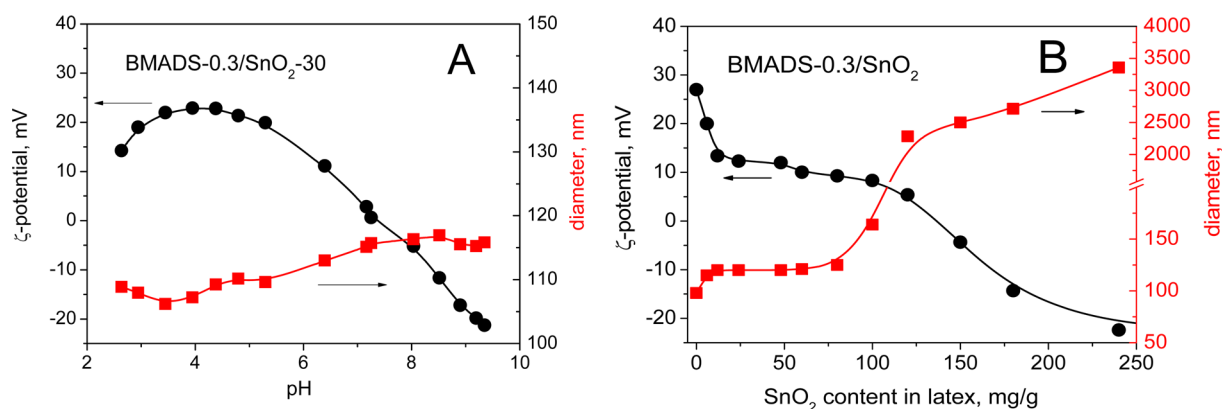
Figure 2. Dependence of electrokinetic potential values (ζ-potential) and particle size of BMADS-0.3/SnO$_2$ composites on pH (A) and amount of SnO$_2$ loaded in the latex, pH 5 (B).

Table 1. Coefficients of ^{57}Co Distribution (K_d) and ^{57}Co Recovery (R) for Latex, Colloidal SnO$_2$, and Latex/SnO$_2$ Composite[a]

media		BMADS-0.3		SnO$_2$		BMADS-0.3/SnO$_2$-30		
		K_d, mL/g	R, %	K_d, mL/g	R, %	K_d (composite),[b] mL/g	K_d (SnO$_2$),[c] mL/g	R, %
CaCl$_2$	0.001 M	0	0	7 080 567	99.1	415 297	13 843 220	99.5
	0.01 M	0	0	1 772 345	96.3	278 372	9 279 079	99.3
	0.10 M	37	1.8	369 015	84.6	37 520	1 250 658	94.9
	0.50 M	77	3.7	200 842	74.4	3909	130 295	66.1

[a]Colloidal SnO$_2$ used for sorption experiments was from the same batch as that used in composite. [b]K_d calculated for total weight of composite. [c]K_d calculated for the weight of SnO$_2$ in composite.
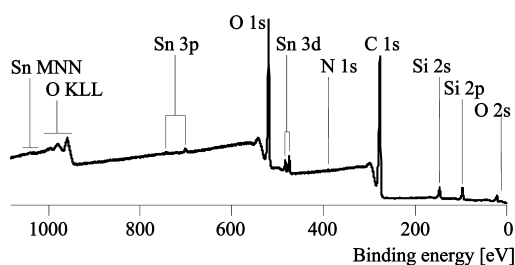

Figure 3. Wide-scan XPS spectrum recorded from BMADS-0.3/SnO$_2$-50 composite coating.
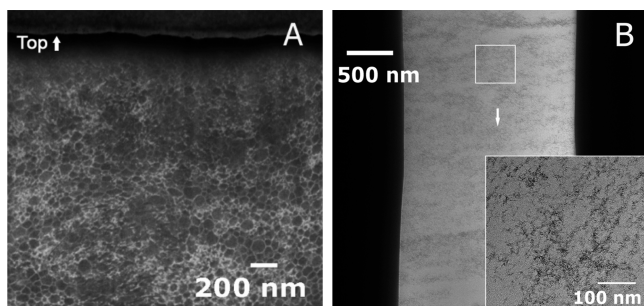

Figure 4. Charge-contrast SEM image (A) and cross-sectional TEM image (B) of BMADS-0.3/SnO$_2$-50 composite coating.

during drying and assures its homogeneous distribution in the coating.

It is important to mention that aggregate formation in the composite film is not beneficial for fixatives, since an inhomogeneous distribution of SnO$_2$ ion-exchange centers within the coatings can reduce their efficiency in cobalt radionuclides entrapment. Taking into account that the colloidal stability of the composite dispersion significantly affects composite latex coatings microstructure,[14] we have limited maximal content of SnO$_2$ in the BMADS-0.3 latex to 50 mg/g, i.e., to the composition which retains high colloidal stability.

Investigations of kinetics of ^{57}Co leaching from the contaminated surface show that the BMADS-0.3 latex coating is highly permeable for Co^{2+} ions: about 50% of ^{57}Co radionuclides were transferred from coated sand to liquid media within the first 30 min of contact and 65% within the first day (Figure 5A). Embedding SnO$_2$ nanoparticles to BMADS-0.3 coatings significantly reduced their permeability. ^{57}Co leaching dropped down to 4.3% when the SnO$_2$ volume fraction in the film was increased up to 4.7% (Figure 5B). The influence of sorbent K_d on composite coating permeability for Co^{2+} ions is clearly illustrated by ^{57}Co radionuclides leaching in solutions with different concentrations of Ca^{2+} ions (Figure 5B). Since the mechanism of Co^{2+} ions sorption on tin oxide is presumably ion exchange,[10,11] Ca^{2+} ions compete with ^{57}Co radionuclides for ion-exchange sites on tin oxide, and the efficacy of ^{57}Co fixation within the BMADS-0.3/SnO$_2$ composite coating decreases with the increase of Ca^{2+} concentration in the leaching media (Figure 5B). Even at the maximum loading of the BMADS-0.3 latex with SnO$_2$ (50 mg/g), ^{57}Co leaching through the composite coatings reaches about 20% after 6 days of contact with 0.1 M solution of CaCl$_2$ (Figure S8, Supporting Information). At the same time span, ^{57}Co leaching with the media with calcium ion concentrations typical for ground waters, i.e., 0.2−4 mM,[15] increased only for 1.5−3% (Figure S8, Supporting Information), which can be still be considered as an indication of satisfactory fixation of cobalt radionuclides on a contaminated surface.

Comparing the data earlier reported for latex/cobalt hexacyanoferrate(II) coatings[7] with the data obtained here for the BMADS-0.3/SnO$_2$ coatings, we can conclude that the
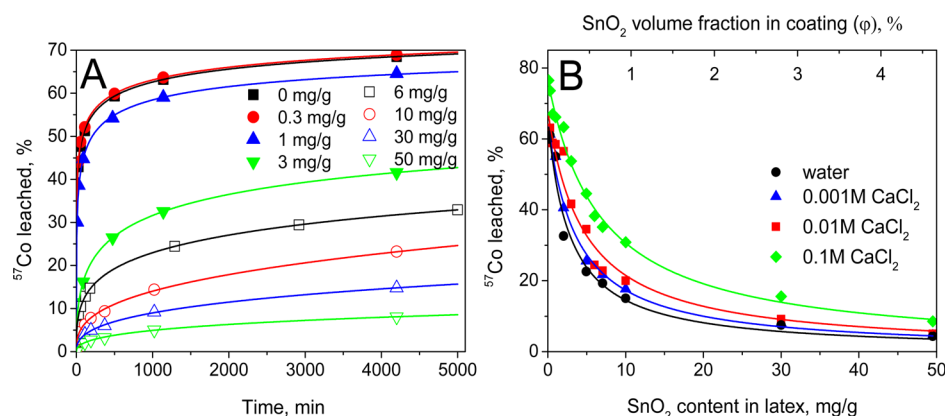
22390

dx.doi.org/10.1021/am5064074 | *ACS Appl. Mater. Interfaces* 2014, 6, 22387−22392

Figure 5. Kinetics of ^{57}Co leaching with 0.01 M CaCl$_2$ solution (A) and dependence of ^{57}Co leaching within 1000 min on composition of leaching media (B) for contaminated quartz sand surface coated with BMADS-0.3/SnO$_2$ composites containing various amount of SnO$_2$ per gram of latex.

distribution coefficients of nanosized sorbents suitable for preparation of composite coatings has to be close to 10^6 mL/g. Only in this case the coatings with a volume fraction of inorganic sorbent up to 5% can efficiently suppress radionuclides leaching from contaminated surface and, thus, eliminate their migration with liquid media.

CONCLUSIONS

Here we have shown that the recently suggested concept of elimination of cesium migration from contaminated surfaces using latex/cobalt hexacyanoferrate(II) composite coatings can be generalized to other radionuclides. Colloidal SnO$_2$ ex-situ synthesized by the sol−gel method was attached to the surface of amino-latex particles to yield latex/SnO$_2$ composite showing selective sorption properties toward cobalt radionuclides. Casting latex/SnO$_2$ composite dispersions containing up to 50 mg of SnO$_2$ per 1 g of the latex on the quartz sand has yielded coherent flawless composite coatings. Despite high hydrophilicity (advancing contact angle 30°) composite coatings with a SnO$_2$ volume fraction of 4.6% reduced ^{57}Co leaching from the contaminated surface to ∼4% compared to 65% leaching from the surface coated with original latex. This allows the conclusion that latex/SnO$_2$ dispersions can be used as dust-suppressing formulations after nuclear accidents to eliminate migration of cobalt and nickel, which has similar chemistry, in the environment with liquid media (atmospheric precipitates, ground waters, etc.).

ASSOCIATED CONTENT

Ⓢ Supporting Information

Dependence of latex and SnO$_2$ particle size on pH; dependence of SnO$_2$ percentage remaining colloidally stable in BMADS-0.3/SnO$_2$ dispersion on the SnO$_2$ content in the latex and TEM image of aminolatex/SnO$_2$ composite; TEM image and particle size distribution for SnO$_2$; particle size distribution for BMADS-0.3/SnO$_2$-30 composite in water and CaCl$_2$ solutions; isotherms of Co(II) sorption on SnO$_2$ and BMADS-0.3/SnO$_2$-50; dependence of the distribution coefficient for ^{57}Co on colloidal SnO$_2$ on pH; kinetics of ^{57}Co recovery; SEM images of BMADS-0.3 and BMADS-0.3/SnO$_2$-50 coatings; high-resolution C 1s XPS spectra; kinetics of ^{57}Co leaching from contaminated quartz sand coated with BMADS-0.3/SnO$_2$-50 composite. This material is available free of charge via the Internet at http://pubs.acs.org.

AUTHOR INFORMATION

Corresponding Author

*Tel.: +7-423-2311889. E-mail: sbratska@ich.dvo.ru.

Author Contributions

The manuscript was written through contributions of all authors. All authors have given approval to the final version of the manuscript.

Notes

The authors declare no competing financial interest.

REFERENCES

(1) Solovitch-Vella, N.; Garnier, J.-M. Comparative Kinetic Desorption of ^{60}Co, ^{85}Sr and ^{134}Cs from a Contaminated Natural Silica Sand Column: Influence of Varying Physicochemical Conditions and Dissolved Organic Matter. *Environ. Pollut.* **2006**, *141*, 98−106.

(2) Schwantes, J. M.; Orton, C. R.; Clark, R. A. Analysis of a Nuclear Accident: Fission and Activation Product Releases from the Fukushima Daiichi Nuclear Facility as Remote Indicators of Source Identification, Extent of Release, and State of Damaged Spent Nuclear Fuel. *Environ. Sci. Technol.* **2012**, *46*, 8621−8627.

(3) Parra, R. R.; Medina, V. F.; Conca, J. L. The Use of Fixatives for Response to a Radiation Dispersal Devise Attack-a Review of the Current (2009) State-of-the-Art. *J. Environ. Radioact.* **2009**, *100*, 923−934.

(4) Chon, J. K.; Lee, K.-J.; Yun, J.-I. Sorption of Cobalt (II) on Soil: Effects of Birnessite and Humic Acid. *J. Radioanal. Nucl. Chem.* **2012**, *293*, 511−517.

(5) Roivainen, P.; Makkonen, S.; Holopainen, T.; Juutilainen, J. Transfer of Elements Relevant to Radioactive Waste from Soil to Five Boreal Plant Species. *Chemosphere* **2011**, *83*, 385−390.

(6) Fox, G. A.; Medina, V. F. Evaluating Factors Affecting the Permeability of Emulsions Used to Stabilize Radioactive Contamination from a Radiological Dispersal Device. *Environ. Sci. Technol.* **2005**, *39*, 3762−3769.

(7) Bratskaya, S.; Musyanovych, A.; Zheleznov, V.; Synytska, A.; Marinin, D.; Simon, F.; Avramenko, V. Polymer-Inorganic Coatings

22391

dx.doi.org/10.1021/am5064074 | *ACS Appl. Mater. Interfaces* 2014, 6, 22387−22392

Containing Nanosized Sorbents Selective to Radionuclides. 1. Latex/ Cobalt Hexacyanoferrate (II) Composites for Cesium Fixation. *ACS Appl. Mater. Interfaces* **2014**, *6*, 16769−16776.

(8) Haas, P. A. Review of Information on Ferrocyanide Solids for Removal of Cesium from Solutions. *Sep. Sci. Technol.* **1993**, *28*, 2479− 2506.

(9) İnan, S.; Koivula, R.; Harjula, R. Removal of [63]Ni and [57]Co from Aqueous Solution Using Antimony Doped Tin Dioxide−Polyacryloni- trile (Sb Doped SnO_2−PAN) Composite Ion-Exchangers. *J. Radioanal. Nucl. Chem.* **2013**, *299*, 901−908.

(10) Misak, N.; Shabana, E.; Mikhail, E.; Ghoneimy, H. Kinetics of Isotopic Exchange and Mechanism of Sorption of Co (II) on Hydrous Stannic Oxide. *React. Polym.* **1992**, *16*, 261−269.

(11) Koivula, R.; Harjula, R.; Lehto, J. Structure and Ion Exchange Properties of Tin Antimonates with Various Sn and Sb Contents. *Microporous Mesoporous Mater.* **2002**, *55*, 231−238.

(12) Musyanovych, A.; Rossmanith, R.; Tontsch, C.; Landfester, K. Effect of Hydrophilic Comonomer and Surfactant Type on the Colloidal Stability and Size Distribution of Carboxyl- and Amino- Functionalized Polystyrene Particles Prepared by Miniemulsion Polymerization. *Langmuir* **2007**, *23*, 5367−5376.

(13) Luo, H.; Cardinal, C. M.; Scriven, L. E.; Francis, L. Ceramic Nanoparticle/Monodisperse Latex Coatings. *Langmuir* **2008**, *24*, 5552−5561.

(14) Sun, J.; Velamakanni, B. V.; Gerberich, W. W.; Francis, L. F. Aqueous Latex/Ceramic Nanoparticle Dispersions: Colloidal Stability and Coating Properties. *J. Colloid Interface Sci.* **2004**, *280*, 387−399.

(15) Schot, P. P.; Wassen, M. J. Calcium Concentrations in Wetland Groundwater in Relation to Water Sources and Soil Conditions in the Recharge Area. *J. Hydrol.* **1993**, *141*, 197−217.